Experimental and numerical analysis of the autoignition behavior of NH3 and NH3/H2 mixtures at high pressure

Dai, Liming; Gersen, Sander; Glarborg, Peter; Levinsky, Howard; Mokhov, Anatoli

Published in:
Combustion and Flame

DOI:
10.1016/j.combustflame.2020.01.023

Publication date:
2020

Combustion and Flame 215 (2020) 134–144

Contents lists available at ScienceDirect

Combustion and Flame

journal homepage: www.elsevier.com/locate/combustflame

Experimental and numerical analysis of the autoignition behavior of NH_3 and NH_3/H_2 mixtures at high pressure

Liming Dai[a], Sander Gersen[b], Peter Glarborg[c], Howard Levinsky[a,*], Anatoli Mokhov[a]

[a] Energy and Sustainability Research Institute, University of Groningen, Nijenborgh 6, 9747 AG Groningen, The Netherlands
[b] DNV GL Oil & Gas, P.O. Box 2029, 9704 CA Groningen, The Netherlands
[c] Department of Chemical and Biochemical Engineering, Technical University of Denmark, Kgs. Lyngby DK-2800, Denmark

ARTICLE INFO

Article history:
Received 20 October 2019
Revised 14 December 2019
Accepted 22 January 2020

Keywords:
Ammonia ignition
Ammonia/hydrogen mixtures
Ignition enhancement
Hydrazine formation
RCM measurements

ABSTRACT

Measurements of autoignition delay times of NH_3 and NH_3/H_2 mixtures in a rapid compression machine are reported at pressures from 20–75 bar and temperatures in the range 1040–1210 K. The equivalence ratio, using $O_2/N_2/Ar$ mixtures as oxidizer, varied for pure NH_3 from 0.5 to 3.0; NH_3/H_2 mixtures with H_2 fraction between 0 and 10% were examined at equivalence ratios 0.5 and 1.0. In contrast to many hydrocarbon fuels, the results indicate that, for the conditions studied, autoignition of NH_3 becomes slower with increasing equivalence ratio. Hydrogen is seen to have a strong ignition-enhancing effect on NH_3. The experimental data, which show similar trends to those observed previously by He et al. (2019) [28], were used to evaluate four NH_3 oxidation mechanisms: a new version of the mechanism described by Glarborg et al. (2018) [29], with an updated rate constant for the formation of hydrazine, $NH_2 + NH_2 (+M) = N_2H_4 (+M)$, and the literature mechanisms from Klippenstein et al. (2011) [30], Mathieu and Petersen (2015) [25], and Shrestha et al. (2018) [31]. In general, the mechanism from this study has the best performance, yielding satisfactory prediction of ignition delay times both of pure NH_3 and NH_3/H_2 mixtures at high pressures (40–60 bar). Kinetic analysis based on present mechanism indicates that the ignition enhancing effect of H_2 on NH_3 is closely related to the formation and decomposition of H_2O_2; even modest hydrogen addition changes the identity of the major reactions from those involving NH_x radicals to those that dominate the H_2/O_2 mechanism. Flux analysis shows that the oxidation path of NH_3 is not influenced by H_2 addition. We also indicate the methodological importance of using a non-reactive mixture having the same heat capacity as the reactive mixture for determining the non-reactive volume trace for simulation purposes, as well as that of limiting the variation in temperature after compression, by limiting the uncertainty in the experimentally determined quantities that characterize the state of the mixture.

1. Introduction

The incentive to reduce the carbon footprint of combustion engines is driving the development and introduction of non-fossil fuels. Ammonia (NH_3) is considered a promising alternative fuel: it is carbon free, can be produced from renewable hydrogen (H_2) and nitrogen from the air (N_2) [1,2] and in liquid form has a relatively high energy density. However, ammonia has different combustion properties compared to common engine fuels, challenging the use of ammonia in engines [3–5]. The significantly lower burning velocity as compared to hydrocarbon fuels (see below) complicates the use of ammonia in the current generation of high-performance reciprocating engines and gas turbines. Also, a significant fraction of the NO_x emissions from ammonia combustion derives from the bound nitrogen in the fuel, diminishing the efficacy of NO_x control strategies based on temperature reduction to mitigate the Zeldovich mechanism. In this regard, very recently Okafor et al. [6] and Karuta et al. [7] showed that rich/lean staged combustion could result in low NO_x emissions from an ammonia-fueled micro gas turbine.

A number of studies have assessed the rate of NH_3 combustion. Burning velocities of NH_3 were determined by Takizawa et al. [8] at atmospheric pressure and by Hayakawa et al. at elevated pressure [9]. The burning velocity of NH_3 is roughly five times lower than that of methane (CH_4). Flow-reactor studies of ammonia oxidation have been performed by Song et al. [10] at high pressures and by Nakamura et al. [11,12] at low pressure in a microflow reactor. A method to enhance the burning velocity is by admixing NH_3 with other fuel molecules that could be considered in this context as

* Corresponding author.
E-mail address: h.b.levinsky@rug.nl (H. Levinsky).

https://doi.org/10.1016/j.combustflame.2020.01.023

"additives", such as H_2 or CH_4. Structures and burning velocities of NH_3 and NH_3/additive-fueled flames, particularly regarding H_2 addition, were reported in [13–17].

However, when considering the use of additives to enhance the burning rate in an engine, one must also be cognizant of the impact of the additive on the autoignition characteristics of the combined fuel. While strongly enhanced autoignition is favorable for use in compression-ignition engines, the negative impact on engine knock can severely limit the utility of the fuel mixture in spark-ignited or dual-fuel (gas) engines.

Ammonia autoignition has been studied in shock tubes [18–26] and Rapid Compression Machines (RCM) [27,28]. The recent studies have reported measurements of the autoignition delay time of NH_3 at elevated pressures more relevant for engine conditions [25–28]. Mathieu and Petersen [25] studied the ignition delay times of NH_3 in a shock tube at pressures up to 30 bar, temperatures of 1560–2455 K, an equivalence ratio (φ) of 0.5, and highly diluted in argon. Shu et al. [26] reported the ignition delay times of NH_3 in shock tube over a temperature range of 1100–1600 K, pressures of 20 and 40 bar, and values of φ = 0.5, 1.0, and 2.0. Pochet et al. [27] measured the ignition delay times of NH_3/H_2 mixtures (0, 10 and 25% vol. H_2) at fuel lean conditions (φ = 0.2, 0.35, 0.5), high pressures (43 and 65 bar) and intermediate temperatures (1000–1100 K) in an RCM. Very recently, He et al. [28] reported the ignition delay times of NH_3 and NH_3/H_2 mixtures (1–20% vol. H_2) measured in an RCM at pressures from 20 to 60 bar, temperatures from 950 to 1150 K, and equivalence ratios from 0.5 to 2. There it was reported that the mechanism from Glarborg et al. [29] showed reasonable agreement for pure NH_3 but underpredicted the ignition delay times for NH_3/H_2 mixtures by up to a factor of 3. In contrast, the mechanism of Klippenstein et al. [30] showed reasonable agreement for NH_3/H_2 mixtures but substantially overpredicted the autoignition delay time of pure NH_3, by more than a factor of 4. We note that the faithful prediction of autoignition delay times for the possible fuel mixtures of ammonia is essential for a reliable assessment of the utility of the fuel in engines.

To gain more insight in the autoignition behavior of NH_3 and NH_3/H_2 mixtures at conditions relevant to practical engines, as well as to provide additional benchmark data for mechanism verification, we report measurements of the ignition delay times of NH_3 and NH_3/H_2 mixtures in an RCM at equivalence ratios varying from 0.5 to 3.0, pressures from 20 to 75 bar, and temperatures in the range 1040–1210 K. We note that the measurements of pure ammonia at pressures above 40 bar and at φ = 2.0 and 3.0 reported here are a significant extension of the test of the chemical mechanism in comparison with previous reports. The hydrogen fraction was varied in the range 0–10%. We compare the measurements with calculations using a modified version of the mechanism of Glarborg et al. [29], as well as with the mechanisms of Klippenstein et al. [30], Mathieu and Petersen [25], and Shrestha et al. [31]. A kinetic analysis was performed to examine NH_3 oxidation under these conditions and the influence of H_2 addition on the ignition process.

2. Experiments and simulations

2.1. Experimental setup

The ignition delay time measurements were performed in an RCM whose details are described in [32,33], and only a brief description will be given here. The gas mixtures were compressed in ~10–20 ms to the peak pressure, with 80% of the compression occurring in less than 3 ms. A creviced piston head was used in this machine to obtain a homogenous reacting core during the experiment [34]. The pressure trace was measured by a Kistler ThermoComp quartz pressure sensor with thermal-shock-optimized construction. The temperature after compression (T_c) was obtained assuming the existence of an adiabatic core, using the following equation, with thermodynamic data from [29]:

$$\int_{T_0}^{T_c} \frac{\gamma(T)}{\gamma(T)-1}\frac{dT}{T} = \ln\left(\frac{P_c}{P_0}\right), \quad (1)$$

where T_0 and P_0 are the initial temperature and pressure, respectively, P_c is the measured pressure after compression and $\gamma(T)$ is the temperature dependent ratio of the heat capacities of the reactants. The compositions (in mole fraction) of the mixtures examined in this study are shown in Table 1. All gas mixtures were prepared in advance in a 10-L gas bottle, used to charge the combustion chamber to the required initial pressure. The mixtures were allowed to mix for least 24 h to ensure homogeneity.

The ignition delay time was defined as the interval between the end of compression and the maximum in the rate of pressure increase during ignition, as illustrated in Fig. 1. The day-to-day reproducibility of the measurements, including repositioning of the piston height, was determined to be better than 5%. The uncertainty of the calculated core gas temperature (T_c) is less than ± 3.5 K for all measurements [35]. We note that the preignition pressure rise reported in [28] was not observed in any of the experiments reported here.

Table 1
Compositions of NH_3 and NH_3/H_2 mixtures studied in this work.

Mixtures	φ	H_2/fuel	NH_3	H_2	O_2	N_2	Ar
Mixture 1	0.5	0	0.118	0	0.176	0	0.706
Mixture 2	0.5	0	0.1	0	0.15	0.1	0.65
Mixture 3	1.0	0	0.143	0	0.107	0	0.75
Mixture 4	2.0	0	0.182	0	0.068	0	0.75
Mixture 5	3.0	0	0.16	0	0.04	0	0.8
Mixture 6	0.5	5%	0.113	0.006	0.176	0	0.705
Mixture 7	0.5	10%	0.109	0.012	0.176	0.141	0.562
Mixture 8	1.0	5%	0.138	0.007	0.107	0.037	0.711

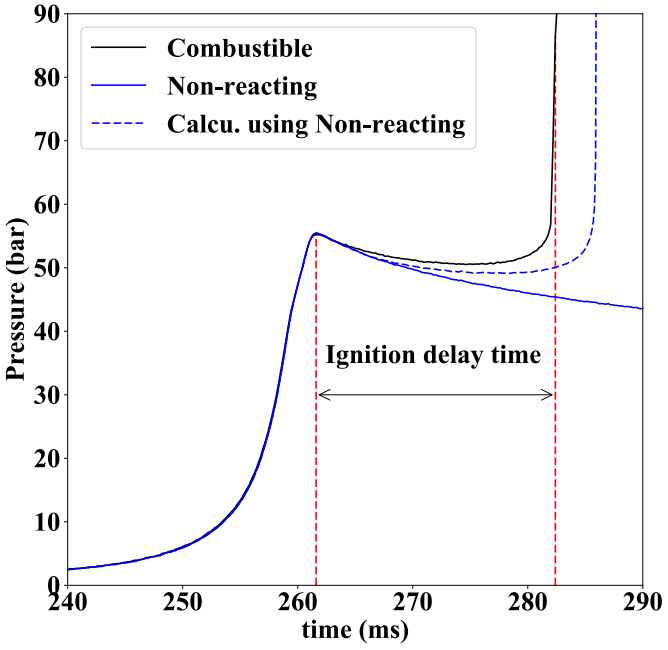

Fig. 1. Example of pressure profiles. Measured combustible mixture (black line) and non-reactive mixture (blue solid line) pressure trace and calculation (blue dashed line) based on non-reactive gas for mixture 1 at T_c = 1080 K, P_c = 55 bar. (For interpretation of the references to color in this figure caption, the reader is referred to the web version of this article.)

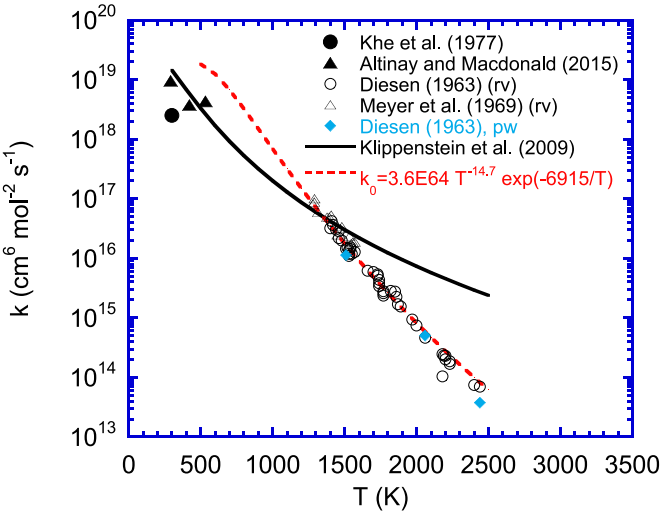

Fig. 2. Data for the low-pressure limit $k_{1b,0}$ of the $NH_2 + NH_2$ (+M) = N_2H_4 (+M) reaction (R1). Symbols denote the experimental data of Khe et al. [37] and Altinay and Macdonald [41] for the forward reaction, and data derived from low-pressure measurements of the reverse rate constant by Diesen [42] and Meyer et al. [43], converted through the equilibrium constant. The solid line shows the theoretical value by Klippenstein et al. [36], while the short-dashed line shows a fit to $k_{1b,0}$, obtained in the present work.

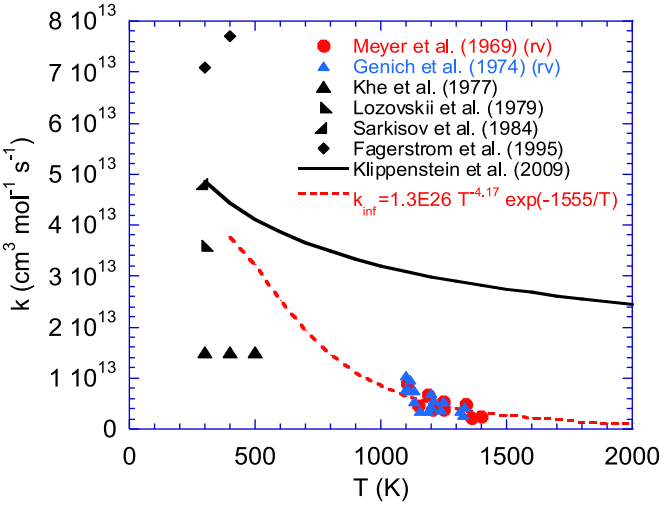

Fig. 3. Data for the high pressure limit $k_{1b,inf}$ of the $NH_2 + NH_2$ (+M) = N_2H_4 (+M) reaction (R1). Symbols denote the experimental data of Khe et al. [37], Lozovskii et al. [38], Sarkisov et al. [39] and Fagerstrom et al. [40] for the forward reaction, and data derived from high-pressure measurements of the reverse rate constant by Meyer et al. [43] and Genich et al. [44], converted through the equilibrium constant. The solid line shows the theoretical value by Klippenstein et al. [36], while the short-dashed line shows a fit to $k_{1b,inf}$, obtained in the present work.

2.2. Numerical approach

The reaction mechanism was drawn largely from the recent review by Glarborg et al. [29]. The H/N/O subset of their mechanism was based on the work by Klippenstein et al. [30], but rate constants for selected key reactions were updated. The amine subset of the kinetic model was intended to describe fuel-N oxidation in combustion, as well as selective non-catalytic reduction of NO with NH_3 (Thermal DeNO$_x$), but the mechanism was not evaluated for ammonia ignition under the high-pressure conditions reported here.

The shock tube work of Mathieu and Petersen [25], conducted at pressures up to 30 bar, indicated that inclusion of an N_2-amine subset involving N_2H_4, following Klippenstein et al. [30], had a detrimental impact on modeling predictions. In the present work, the rate coefficients for the reaction forming hydrazine, $NH_2 + NH_2$ (+M) = N_2H_4 (+M) (R1), were re-evaluated. Both Glarborg et al. [29] and Klippenstein et al. [30] relied on the theoretical work of Klippenstein et al. [36], which was in good agreement with the low-temperature measurements of the reaction [37–41]. At elevated temperature, the reaction has been studied over a wide range of pressure in shock tubes. Diesen [42] and Meyer et al. [43] report data, presumably at the low-pressure limit. Kinetic modeling of the experiments of Diesen [42] indicates that $k_{1b,0}$ is roughly 1/3 of the observed disappearance rate for N_2H_4, since both the amino radicals formed in the dissociation act to remove hydrazine. The rate constant reported by Diesen [42] has thus been reduced by a factor of three. Similarly, the rate constants reported by Meyer et al. [43] were multiplied by a factor of 2/3. Fig. 2 compares data for the low-pressure limit of R1; i.e., the low-temperature experimental data of Khe et al. [37] and Altinay and Macdonald [41], the theoretical value by Klippenstein et al. [36], and data derived from low-pressure measurements of the reverse rate constant by Diesen [42] and Meyer et al. [43], converted through the equilibrium constant.

The data in Fig. 2 indicate that the low-pressure limit by Klippenstein et al. [36] agree well with the low-temperature data for the forward reaction and also with results for R1b at around 1500 K, but at higher temperatures the value from Klippenstein et al. appears to overpredict the recombination rate. Fig. 3 shows results obtained at high pressure, presumably at the high-pressure limit. Data for the forward reaction, obtained at low temperature by Khe et al. [37], Lozovskii et al. [38], Sarkisov et al. [39] and Fagerstrom et al. [40] are scattered, varying almost an order of magnitude. The results derived from the high-temperature measurements by Meyer et al. [43] and Genich et al. [44] are in good agreement, but indicate a high-pressure limit somewhat smaller than calculated by Klippenstein et al. [36].

The reason for the discrepancy between the theoretical rate coefficients for $NH_2 + NH_2$ (+M) = N_2H_4 (+M) and the shock tube measurements of the reverse step is not known at present. The heat of formation of N_2H_4 has been in question, but the current value [29] is in excellent agreement with the recent recommendations by Dorofeeva et al. [45] and Feller et al. [46]. It is an issue whether the experimental data are truly obtained at the low- and high-pressure limits, respectively, but more work is required to resolve this issue. Under the conditions of the present work, the modification of the rate constant for R1 turns out to have only a limited impact on ignition delay predictions, calculations with the mechanism of Glarborg et al. [29] are largely within 10% of those using the modified mechanism; consequently, only the latter are shown.

The ignition delay times for the conditions in the RCM were simulated using the homogenous reactor code from the Cantera package [47]. To account for changes in the mixture conditions during compression and post-compression heat loss, the specific volume of the adiabatic core was used as input into the simulations. The specific volume was derived from the measured pressure trace of a non-reactive gas mixture that had the same average heat capacity as the combustible mixture. An illustration of the measured and simulated pressure profiles at T_c = 1100 K, P_c = 55 bar is shown in Fig. 1. As will be discussed below, using a mixture having the average heat capacity for the measured non-reactive trace, as opposed to the common practice of replacing the oxygen in the mixture by nitrogen, can impact the reliability of the simulations.

2.3. Sensitivity and flux analyses

Sensitivity analyses were performed to identify the most important reactions controlling the autoignition behavior. Sensitivity

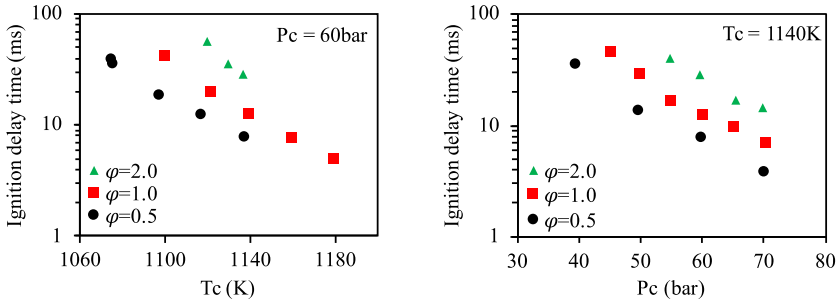

Fig. 4. Effect of equivalence ratio on ignition delay time for pure NH_3 at φ = 0.5 (mixture 2), 1.0 and 2.0. (a) measurements varying T_c at constant P_c (isobars), (b) measurements varying P_c at constant T_c (isotherms). Note: the error bars of ignition delay times (± 5%) are covered by the symbols and are thus not visible in the figures.

coefficients (S) were obtained using:

$$S = \frac{(\Delta\tau/\tau)}{(\Delta k_i/k_i)}, \tag{2}$$

where $\Delta\tau$ is change of ignition delay time corresponding to change of rate constant Δk_i. A negative coefficient S indicates promoting effect (reducing ignition delay time when a rate constant is increased) and a positive coefficient denotes inhibiting effect (increasing ignition delay time when a rate constant is increased). Flux analyses were performed at the point of 20% fuel consumption to study reaction path at the experimental conditions [48].

3. Results and discussion

3.1. Pure NH_3 mixtures

The ignition delay times of pure NH_3 measured at $\varphi = 0.5, 1.0$ and 2.0 are shown in Fig. 4. As can be seen, the ignition delay times decrease with increasing temperature and pressure at all equivalence ratios. The data for isobars and isotherms indicate a significant increase in ignition delay time with equivalence ratio, by a factor of two when going from 0.5 to 1 and from 1 to 2. We note that the substantial differences in measured ignition delay times for equivalence ratios 0.5 and 1.0 reported here were not observed in [28]. However, the interpretation of this functional dependence for practical devices is complicated by the change in $(Ar+N_2)/O_2$ ratio that was necessary to reach the ignition temperatures under these condition of pressure, as is often done in ignition studies (see, for example, [25,28,49]). We consider the possible impact of the changes in inert/oxygen ratio below.

The measured ignition delay times of pure NH_3 were used to evaluate the performance of the four mechanisms referred to above at $\varphi = 0.5, 1.0, 2.0$ and 3.0, as shown in Fig. 5. The mechanism from the present study, drawn from Glarborg et al. [29] with the modification described in Section 2.2, predicts the ignition delay times well at all conditions, with a maximum deviation less

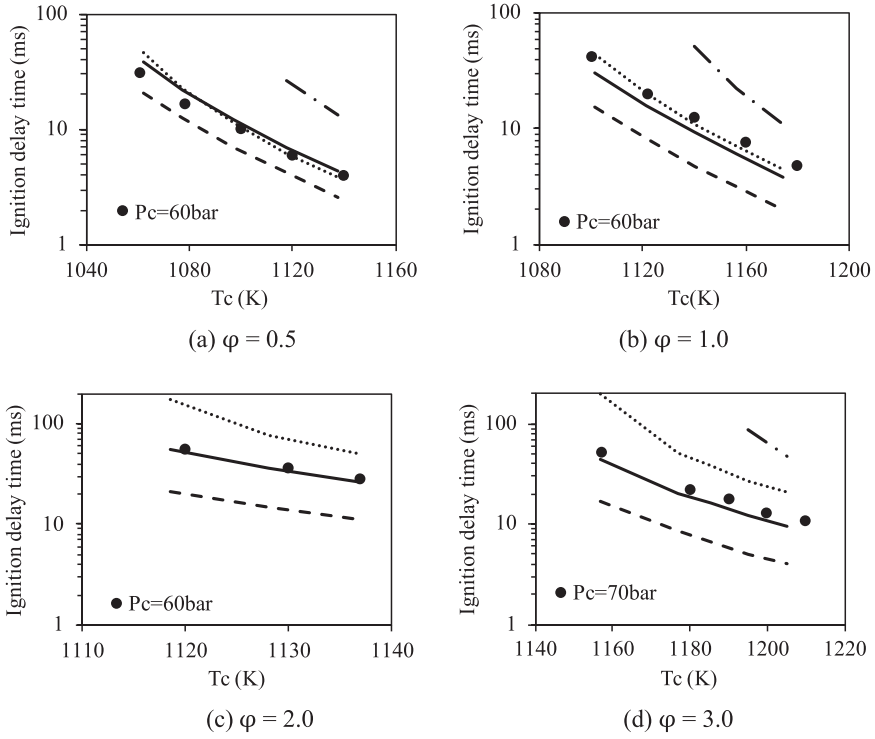

Fig. 5. Measured (points) and calculated (lines) ignition delay times of NH_3 as function of temperature at φ = 0.5 (mixture 1), 1.0, 2.0 and 3.0. Solid lines: the mechanism presented here, dashed lines: the Shrestha et al. mechanism [31], dotted lines: the Mathieu and Petersen mechanism [25], and dash-dot lines: the Klippenstein et al. mechanism [30]. (The small apparent mismatches in temperature between some experimental and calculated data arise from slight differences in temperature between the reactive and non-reactive experiments.).

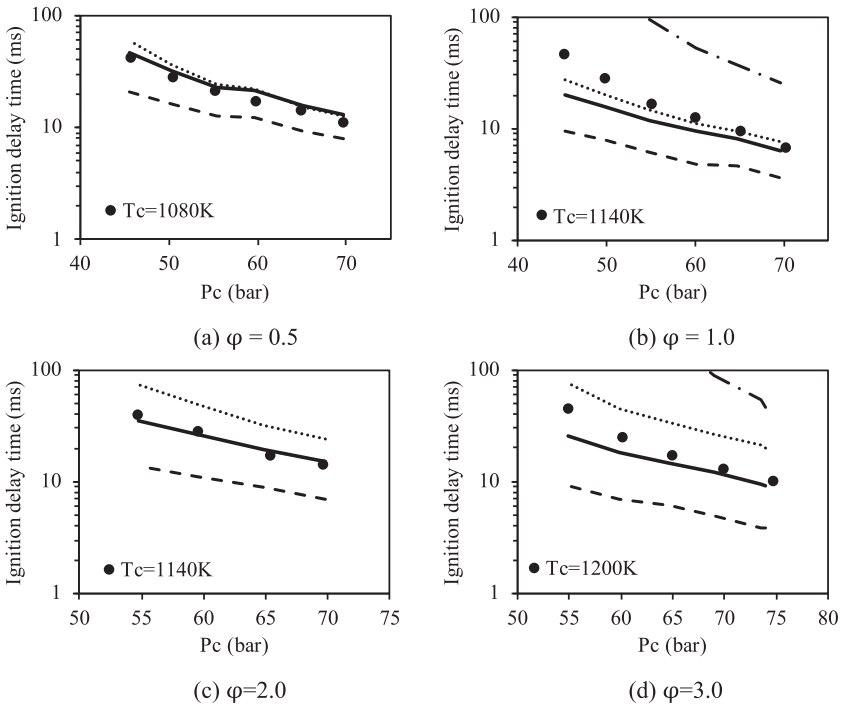

Fig. 6. Measured (points) and calculated (lines) ignition delay times of NH_3 as function of pressure at $\varphi = 0.5$ (mixture 1), 1.0, 2.0 and 3.0. Solid lines: the mechanism in this work, dashed lines: the Shrestha et al. mechanism [31], dotted lines: the Mathieu and Petersen mechanism [25] and dash-dot lines: the Klippenstein et al. mechanism [30].

than 30%. The agreement under lean conditions marks a departure from the results reported in He et al. [28], who noted a significant underprediction, more than a factor of 2, with the mechanism from [29]; as indicated above, the differences between the mechanism in [29] and that used here do not account for this discrepancy (see below). The model from Shrestha et al. [31] shows underprediction for all conditions, by factors of ~1.5, 2, 2 and 3 at $\varphi = 0.5$, 1.0, 2.0 and 3.0, respectively. The Mathieu and Petersen mechanism [25] yields good predictions at $\varphi = 0.5$ (again in contrast with [28]) and 1.0, with deviation less than 20%; however, it overpredicts the ignition delay times by a factor of ~2 at $\varphi = 2.0$ and 3.0. The model from Klippenstein et al. [30] overpredicts the ignition delay times by more than a factor of 4 at $\varphi = 0.5$, 1.0 and 3.0 and fails to predict ignition at $\varphi = 2.0$. The overprediction reported here is in agreement with the observations in [28].

Fig. 6 illustrates the measured ignition delay times as a function of pressure at $\varphi = 0.5$, 1.0, 2.0 and 3.0, at fixed T_c = 1080 K, 1140 K, 1140 K and 1200 K, respectively. As noted above, the ignition delay time decreases with increasing P_c at all four equivalence ratios. The present mechanism predicts the ignition delay times very well at $\varphi = 0.5$ and 2.0, with deviations below 25%. However, at $\varphi = 1.0$ and 3.0, good agreement is obtained only at high pressures, while at lower pressure the ignition delay is underpredicted by up to 60%. The Shrestha et al. [31] mechanism again shows underprediction by more than a factor of 2 at all conditions. Mathieu and Petersen's mechanism [25] yields similar predictions as the present model at $\varphi = 0.5$ and 1.0, but overpredicts the ignition delay times by factors of ~2 at $\varphi = 2.0$ and 3.0. The model from Klippenstein et al. [30] shows overprediction by a factor of 4 at $\varphi = 1.0$ and 3.0 and fails to predict ignition at $\varphi = 0.5$ and 2.0 for these pressures and temperatures. In general, the present mechanism, based on Glarborg et al. [29], has the best performance in predicting ignition delay times of pure NH_3 in the range of equivalence ratio $\varphi = 0.5$–3.0 for the pressures and temperatures used here.

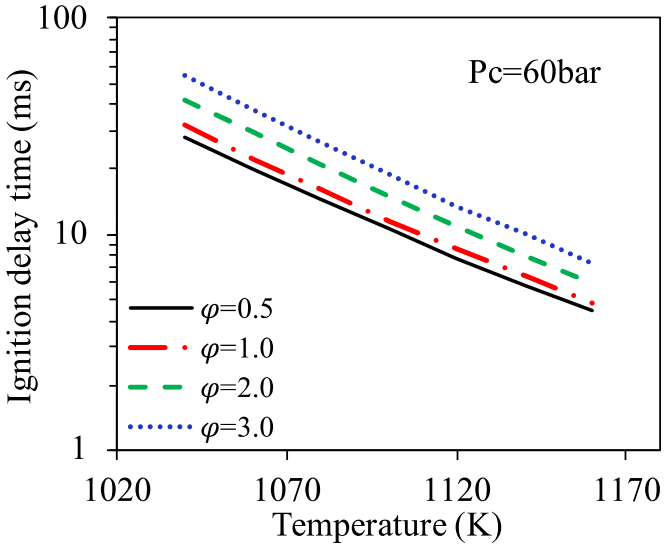

Fig. 7. Calculated ignition delay times of pure NH_3 using the mechanism presented here at a constant Ar/O_2 ratio of 5.

Given the agreement between the experiments and the simulations using the current mechanism, we can disentangle the effects of varying inert/O2 ratio from those of the change in equivalence ratio mentioned above. In Fig. 7, we show the equivalent data for Fig. 4a, but using a constant Ar/O_2 ratio of 5. These results show that, while the effect of inert/O_2 ratio seen in Fig. 4 is substantial, the ignition delay time for ammonia increases with equivalence ratio, in contrast with the ignition of many hydrocarbons (see, for example, [32,50]).

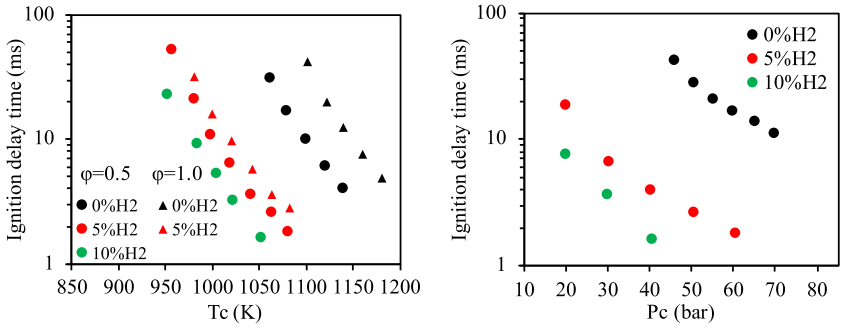

(a) φ = 0.5 and 1.0, P_c = 60 bar (b) φ = 0.5, T_c = 1080 K

Fig. 8. Effect of H_2 addition on the ignition delay times at $\varphi = 0.5$ (circles) and $\varphi = 1.0$ (triangles). (a) isobars, (b) isotherms.

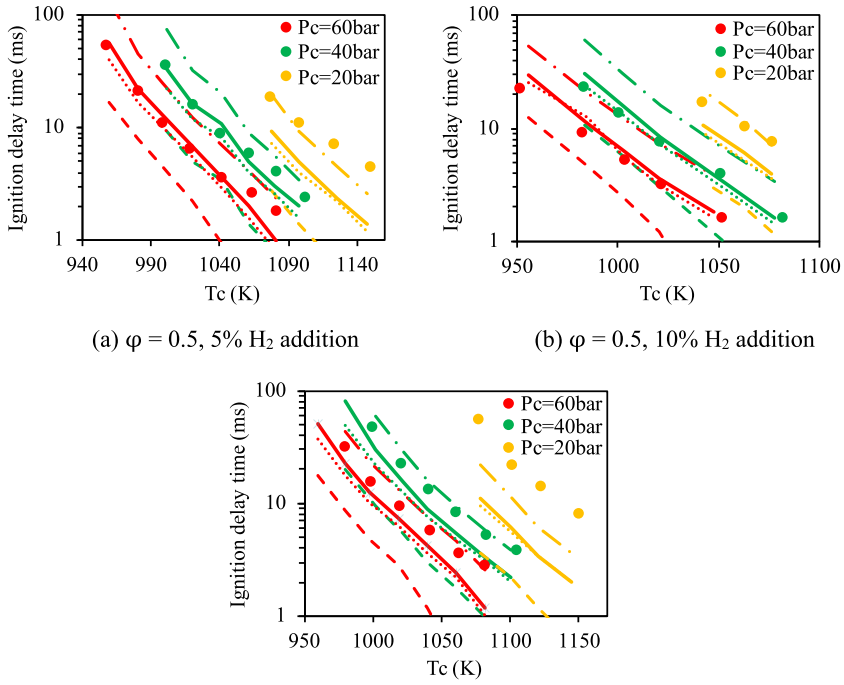

(a) φ = 0.5, 5% H_2 addition (b) φ = 0.5, 10% H_2 addition

(c) φ =1.0, 5% H_2 addition

Fig. 9. Measured (points) and calculated (lines) ignition delay times as function of temperature for mixture 5% H_2, $\varphi = 0.5$ (a), 10% H_2, $\varphi = 0.5$ (b) and 5% H_2, $\varphi = 1.0$ (c). Solid lines: using the mechanism in this work, dashed lines: the Shrestha et al. mechanism [31], dotted lines: the Mathieu and Petersen mechanism [25] and dash-dot lines: the Klippenstein et al. mechanism [30].

3.2. NH_3/H_2 mixtures

Experiments with three NH_3/H_2 mixtures (5% and 10% H_2 addition at $\varphi = 0.5$ and 5% H_2 addition at $\varphi = 1.0$) were conducted to characterize the impact of H_2 on the ignition delay and to further evaluate the performance of the mechanisms. As reported by others [28], Fig. 8 shows a significant ignition-enhancing effect of H_2. At $\varphi = 0.5$, the ignition delay times of both isobars (Fig. 8a) and isotherms (Fig. 8b) are reduced by a factor of ~12 when H_2 addition increases from 0 to 5% of the fuel mixture, and by an additional factor of ~2 when increasing the H_2 fraction from 5% to 10%. At $\varphi = 1.0$, 5% H_2 addition to NH_3 leads to a reduction of the ignition delay times by a factor of ~28, indicating that the ignition-enhancing effect of H_2 addition is more pronounced at higher φ.

The NH_3/H_2 measurements were extended to P_c = 40 and 20 bar, as shown Figs. 8b and 9. For all three mixtures, the ignition delay times decrease with increasing pressures. At $\varphi = 0.5$ (Fig. 8b and 9a/b) for both 5% and 10% H_2 addition, increase of P_c from 20 bar to 40 bar and from 40 bar to 60 bar leads to reduction of the ignition delay times by factors of ~4.5 and ~2.5, respectively. A similar trend is found at $\varphi = 1.0$ (Fig. 9c), again with a factor of ~2.5 between P_c = 40 and 60 bar, but with a larger factor, of ~6, between P_c = 20 and 40 bar.

The agreement of the calculations using the present mechanism with the measurements for the isobars at P_c = 40 bar and 60 bar is generally within 30%. At P_c = 20 bar, an underprediction by a factor ~2 is observed for both hydrogen fractions at $\varphi = 0.5$ (Fig. 9a and b) and by a factor of 4.5 for 5% H_2 at $\varphi = 1.0$. The Shrestha et al. mechanism [31] underpredicts the ignition delay times by a factor of ~2.5 for isobars at P_c = 40 and 60 bar and by a factor of ~10 at P_c = 20 bar for all three H_2-containing mixtures. Predictions with the model from Mathieu and Petersen [25] are close to those using the mechanism of the present study. The Klippenstein et al. mechanism [30] yields an overprediction by a factor ~2 for isobars at $\varphi = 0.5$, P_c = 40 and 60 bar, whereas the deviation for the isobars at P_c = 20 bar is less than 40%. At $\varphi = 1.0$, this mechanism predicts ignition delay times within ~20% for isobars at P_c = 40 and 60 bar, while an underprediction by a factor ~2 is observed at P_c = 20 bar. Overall, for the NH_3/H_2 mixtures studied in this work, the present mechanism and that of Math-

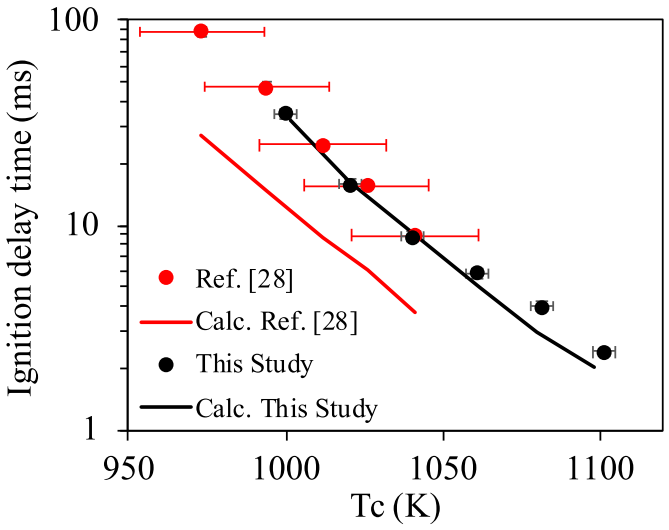

Fig. 10. Comparison between the measurements from He et al. [28] and this study at $\varphi = 0.5$, 5% H_2 addition, $P_c = 40$ bar. (For explanation of the error bars, see text.).

ieu and Petersen [25] show the best performance at high pressure ($P_c = 40$ and 60 bar), while the Klippenstein et al. mechanism [30] yields better results at low pressures ($P_c = 20$ bar). The mechanism from Shrestha et al. [31] tends to underpredict ignition delay times at all conditions. While the simulation results under similar conditions as reported in [28] show close agreement between the mechanisms of Glarborg et al. [29] and Mathieu and Petersen [25] for all mixtures studied, they do not observe the good agreement for these mechanisms with the experimental results for NH_3/H_2 mixtures at 40 bar observed here. Also, while we note the improved predictions for the mechanism of Klippenstein et al. [30] at 20 bar and lean conditions (Fig. 9a and b), the agreement in [28] with the measurements under the same conditions is significantly poorer. We return to possible origins of these differences below.

3.3. Comparison with previous RCM measurements

As mentioned in the introduction, very recently He et al. [28] also reported ignition delay time measurements for NH_3/H_2 mixtures. They found that the mechanism from Glarborg et al. [29] underpredicts the ignition delay times for NH_3/H_2 mixtures compared to their measurements. For instance, an underprediction by a factor of ~3 was observed at $\varphi = 0.5$, $P_c = 40$ bar with 5% H_2 addition (Fig. 5c in [28]). The ignition delay times measured for the same conditions in this study are consistent with those measured by He et al. [28]. However, as shown in Fig. 10, calculated ignition delay times using the current mechanism (with marginal differences in computed delay times compared with those obtained using Glarborg et al. [29]) agree to better than 30% with the ignition delay times measured under the same conditions.

Since the ignition delay times were simulated using pressure traces derived from non-reactive mixtures, we noticed a difference in the way in which the non-reactive experiments were performed between [28] and the method used here, which may contribute to the observed differences. In [28], as well as in [48,49,51], the non-reactive experiments were conducted by replacing the O_2 in the combustible mixtures with the same fraction of N_2. Because N_2 has slightly smaller heat capacity than O_2, this leads to larger ratios of the heat capacities and thus to higher T_c in the non-reactive experiments than in the reactive mixture. For example, a set of measured pressure traces and the derived volume traces for 'mixture 5b' in [28] were provided to us by the authors of [28], shown in Fig. 11. The non-reactive pressure and volume traces show differences with the reactive traces. The equivalent non-reactive temperature history for this example give T_c roughly 15 K higher than that derived from the measured profile. In the present study, rather than replacing the oxygen by nitrogen to yield the unreactive mixture, the difference in the heat capacities between O_2 and N_2 were considered: the N_2 fraction was adjusted (to be slightly larger than that of the O_2 being replaced, with a corresponding reduction in the Ar fraction) to give the same average ratio of the heat capacities as in the reactive mixture. This results in a faithful duplication of the peak pressure and pressure decrease after compression but prior to ignition as shown in Fig. 12. The differences in computed temperature after compression (T_c) were less than 1 K in this case. When using the reactive mixture heat capacity in the non-reactive volume trace from [28], the pressure trace still shows the same discrepancy with the measured reactive trace, but the error in the maximum temperature is reduced to roughly 4 K. (We note that the 4 K inconsistency when simply replacing oxygen by the same fraction of nitrogen is specific for this example; under other conditions, the inconsistency could be significantly different. We are currently quantifying this aspect further and will report it in a methodological assessment.) Although significant, the 4 K for this example is still not enough to account for the differences in simulated results observed in the present comparison. A direct comparison of the reactive pressure traces in Figs. 11 and 12 (visible in the insets in these figures) shows that the pressure (and coupled to it the temperature) after compression in the profile from [28] is nearly constant until ignition, while the pressure profile measured here decreases significantly after compression. Since T_c in both mixtures is reported to be the same, it is not physically reasonable for these two profiles to give the same ignition delay time.

We note that the supplementary material in [28] discusses the uncertainties in the experimental conditions, particularly initial temperature and pressure after compression, that result in a net uncertainty in T_c of 10–20 K. In Fig. 10 this uncertainty in the measurement conditions is reflected, using error bars of ±20 K as an example. As shown in [28], this results in an uncertainty in the computed ignition delay time of roughly a factor of three; Fig. 10 shows that a difference of 20 K in T_c is enough to bring the measured and simulated ignition delay times reported in [28] to within ~50%. In the current report, the measured quantities are ascertained to yield the resultant ± 3.5 K [35] uncertainty in T_c noted above and indicated by the error bars in Fig. 10. This uncertainty in T_c translates into an uncertainty in the computed ignition delay times of 5–10%. The differences in the pressure profiles for similar reported experimental conditions and uncertainty in the temperature after compression argue for caution when regarding the apparent excellent agreement between the experimental results suggested by the points neglecting the error bars seen in Fig. 10. Inclusion of the error bars for T_c facilitates the quantitative interpretation of the degree to which simulations and measurements are consistent.

Based on these observations, we emphasize the importance of matching the heat capacity of the reactive mixture when determining the volume profile from the non-reactive mixture, indicating the uncertainty in T_c and reducing the uncertainty in the quantities that determine T_c when quantitatively assessing the agreement between experimental and simulated ignition delay times for the purposes of mechanism evaluation.

3.4. Kinetic analysis

To analyze the effect of H_2 addition on the ignition delay times, a sensitivity analysis using the current mechanism was performed. The sensitivities at $\varphi = 0.5$, $T_c = 1080$ K, $P_c = 60$ bar with H_2

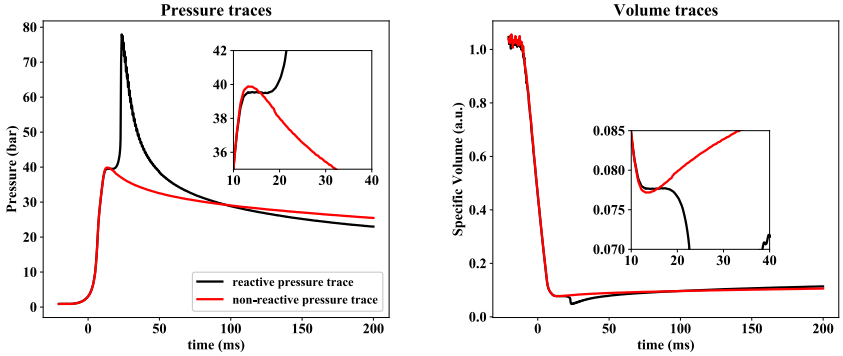

Fig. 11. Pressure traces of combustible (black) and non-reactive (red) gas of 'mixture 5b' from [28] measured at T_c = 1041.2 K, P_c = 39.5 bar and temperature and specific volume traces derived from pressure traces. (For interpretation of the references to color in this figure caption, the reader is referred to the web version of this article.)

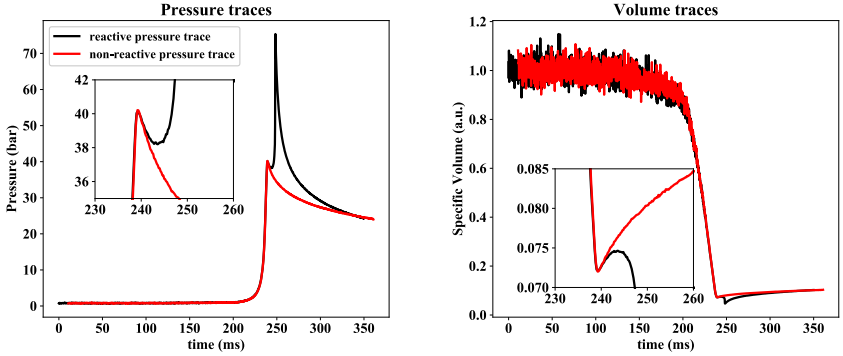

Fig. 12. Pressure traces of combustible (black) and non-reactive (red) gas of 'mixture 6' of this study measured at T_c = 1040.5 K, P_c = 40.1 bar and temperature and specific volume traces derived from pressure traces. (For interpretation of the references to color in this figure caption, the reader is referred to the web version of this article.)

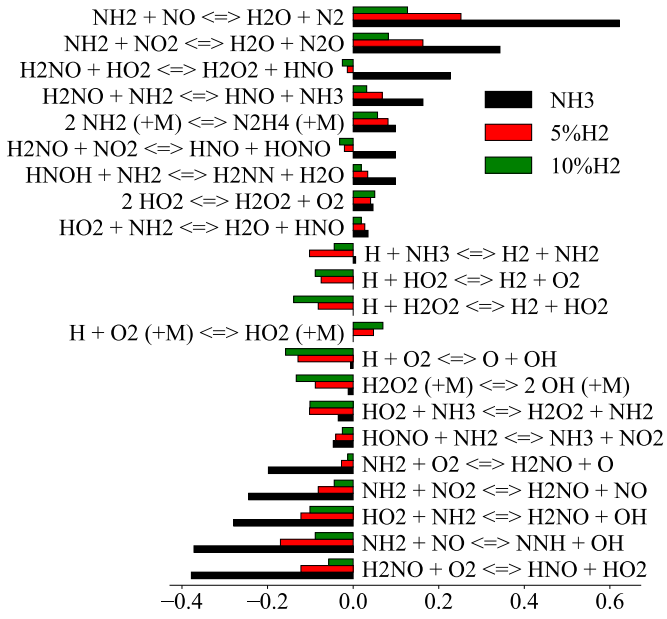

Fig. 13. Sensitivity analysis for the ignition delay time of NH_3 with 0, 5 and 10% H_2 addition at φ = 0.5, T_c =1080 K, P_c = 60 bar.

fractions of 0, 5 and 10% H_2 are shown in Fig. 13. The most important reaction promoting ignition for pure NH_3 under these conditions is $H_2NO + O_2 = HNO + HO_2$, followed by $NH_2 + NO = NNH + OH$ and reactions of NH_2 with HO_2, NO_2 and O_2 producing reactive intermediates and radicals like H_2NO, OH, O and NO. Oxygen is directly involved in the oxidation of H_2NO and NH_2, and in the formation of NO; these reactions will be promoted if more O_2 is provided, resulting in shorter ignition delay times, consistent with the results measured in leaner mixtures as shown in Fig. 4. The most inhibiting reactions are the terminating steps $NH_2 + NO = H_2O + N_2$ and $NH_2 + NO_2 = H_2O + N_2O$, which compete with the promoting reactions $NH_2 + NO = NNH + OH$ and $NH_2 + HO_2 = H_2NO + OH$. The competition between these reactions is discussed in detail in [30].

With H_2 addition, key reactions involved in the H_2/O_2 mechanism become important, including the competition between $H + O_2 = O + OH$ and $H + O_2 (+M) = HO_2 (+M)$, for which the ignition of pure ammonia exhibits virtually no sensitivity. The dissociation of H_2O_2, $H_2O_2 (+M) = 2OH (+M)$, becomes the second most important ignition-enhancing reaction at a relatively modest 10% H_2 in the fuel. We also observe the increased sensitivity of ignition to $HO_2 + NH_3 = H_2O_2 + NH_2$ upon hydrogen addition as compared to pure ammonia. Note that while hydrazine formation is an important step in ammonia oxidation, Fig. 13 indicates a sensitivity of at most ~10%, consistent with the observation that the changes in the rate constant for this reaction presented in Section 2.2 has only a modest effect on the ignition delay time as compared with the mechanism in [29].

Fig. 14 shows the most sensitive reactions for pure NH_3 and NH_3 with 5 and 10% H_2 addition at φ = 1.0, T_c = 1080 K, P_c = 60 bar. The most sensitive reactions for pure NH_3 at φ = 1.0 are identical to those for pure NH_3 at φ = 0.5. The reactions $H + O_2 = O + OH$ and $H_2O_2 (+M) = 2OH (+M)$ remain important for H_2 addition at φ = 1.0. Interestingly, at 5% H_2 addition the reaction $H + NH_3 = H_2 + NH_2$, which gives no sensitivity at φ = 0.5, is seen to be ignition enhancing addition at the same level of sensitivity as the branching reaction between NH_2 and HO_2, while at 10% H_2 the sensitivity all but vanishes. These results suggest that, under stoichiometric conditions, the shortage of hydrogen enhances the importance of $H+NH_3=H_2+NH_2$. While the

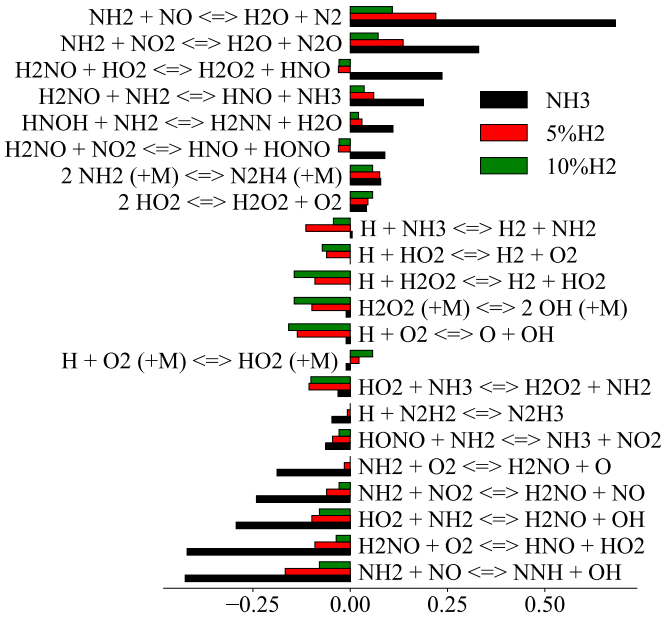

Fig. 14. Sensitivity analysis for the ignition delay time of NH_3 with 0, 5 and 10% H_2 addition at φ = 1.0, T_c =1080 K, P_c = 60 bar.

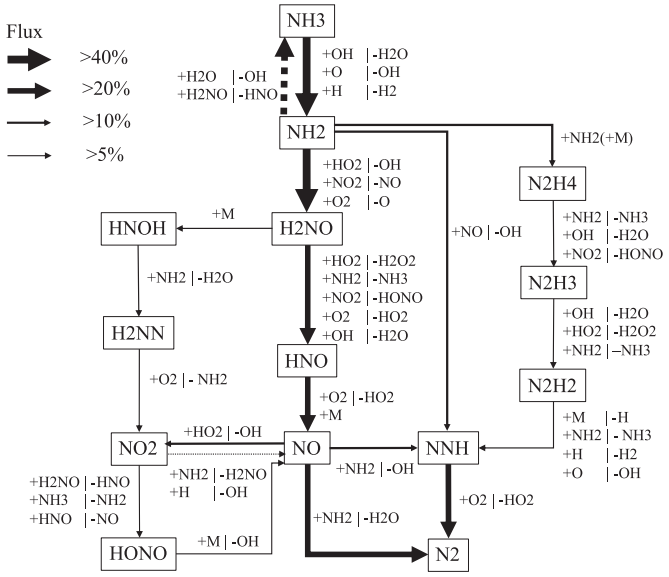

Fig. 15. Reaction path diagram for pure NH_3 at φ = 0.5, T_c =1080 K, P_c = 60 bar.

sensitivities observed for the conditions here (60 bar) are qualitatively similar to those reported in [28] (up to a maximum pressure of 40 bar), there are some differences in the relative ranking. Since the sensitivity analyses in [28] appear to be normalized (while here they are not), and with no details as to how the analyses were performed, we refrain from a detailed comparison with the analysis presented there. We do note that in [28] the mechanism from [29] shows H + NH_3 = H_2 + NH_2 as ignition inhibiting at 20% H_2 in the mixture, in contrast to the ignition-enhancing behavior observed here at lower H_2 fractions.

The reaction path of pure NH_3, calculated using the current mechanism, is shown in Fig. 15. Fluxes lower than 5% are not shown to avoid clutter. As can be seen, ammonia is primarily consumed by O, H and OH radicals, producing the amine radical NH_2. The NH_2 radical is partly converted into NO in the sequence $NH_2 \xrightarrow{+HO_2,NO_2} H_2NO \xrightarrow{+O_2} HNO \xrightarrow{+O_2} N$. Nitric oxide then reacts with NH_2 through either $NH_2 \xrightarrow{+NO} N_2$ or $NH_2 \xrightarrow{+NO} NNH \xrightarrow{+O_2} N_2$. The NH_2 radical can also recombine to form hydrazine (N_2H_4), followed by sequential H abstraction to form N_2. (The reaction path of NH_3 with 10% H_2, included in the Supplementary Material, shows that 10% H_2 addition had no significant influence on the NH_3 oxidation paths). While the major paths observed here are similar to those reported in [28], using the mechanism in [29], we note that the route via hydrazine has been left out of the analysis in [28]. However, the path to hydrazine formation changes the routing of NH_2 by only 10% under the conditions described here.

To obtain a better understanding of the effect of H_2 addition on ignition, the species histories for H_2O_2, HO_2, OH and H in the period leading to ignition for pure NH_3 and for 10% H_2 addition were calculated using the current mechanism, shown in Fig. 16. For this purpose, the calculations are performed as constant volume simulations. As can be seen, with 10% H_2 addition, hydrogen peroxide H_2O_2 and HO_2 accumulate before ignition to a fraction that is ~10 times higher than when igniting pure NH_3. This results in a faster buildup of the radical pool, particularly for OH. Similar species histories were found at φ = 1.0 (included in the Supplementary Material). Clearly, with only modest hydrogen addition the fractions of species that are important for the ignition in fuels dominated by the H_2/O_2 mechanism are drastically increased.

4. Conclusions

The autoignition behavior of NH_3 and NH_3/H_2 was studied in a RCM at φ ranging from 0.5 to 3.0, pressures from 20 to 75 bar, temperatures from 1040 to 1210 K, and with H_2 addition in the range 0–10%. In contrast to many hydrocarbon fuels [32,50], the ignition delay time of pure NH_3 increases with equivalence ratio.

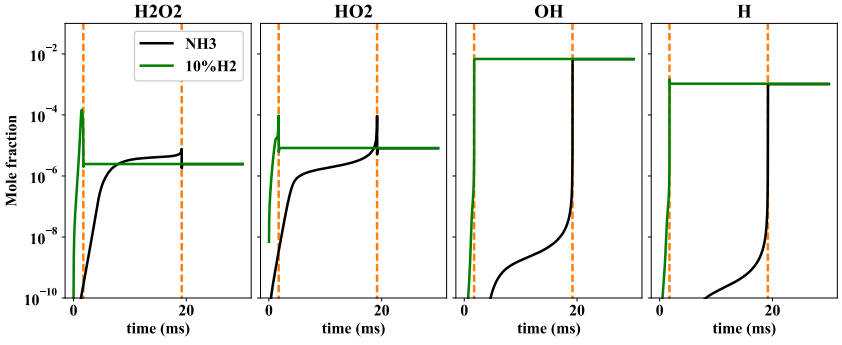

Fig. 16. Selected species history in ignition of NH_3 (black lines) and NH_3 with 10% H_2 addition (green lines) at φ = 0.5, T_c = 1080 K, P_c = 60 bar. Orange dashed line –time at which ignition occurred in the simulations. (For interpretation of the references to color in this figure caption, the reader is referred to the web version of this article.)

Hydrogen addition has a significant ignition-enhancing effect on NH_3, with 5% H_2 addition reducing the ignition delay times by a factor of ~28 at $\varphi = 1.0$. Comparison of the present experimental data with a mechanism described here and mechanisms from Klippenstein et al. [30], Mathieu and Petersen [25] and Shrestha et al. [31] are used to evaluate their veracity in predicting ignition delay times under the conditions reported here. The mechanism from this study has the best performance, yielding predictions for both pure NH_3 and NH_3/H_2 mixture at high pressures (40–60 bar) that are generally within 40% of the experimental results.

Sensitivity analysis of ignition delay times using the present mechanism indicates the importance of O_2 in the oxidation of H_2NO and NH_2; increasing O_2 by decreasing the equivalence ratio suggests the trend of shortening of the ignition delay times observed in the measurements. The addition of modest hydrogen fractions decreases the importance of these reactions in favor of the reactions from the H_2/O_2 mechanism, particularly $H + O_2 = OH + O$ and $H_2O_2 (+ M) = 2OH (+ M)$. Given the limited computed sensitivity of the recombination of NH_2 to hydrazine, the change in rate constant reported here results in modest changes in the simulated ignition delay times as compared with the mechanism used in [29]. Calculated species histories show an increase in the preignition fractions of hydrogen peroxide H_2O_2 and HO_2 by a factor of 10 with 10% H_2 in the fuel as compared with pure NH_3, consistent with the strong ignition-enhancing effect of hydrogen at low fractions.

We further indicate the importance of matching the heat capacities of the non-reactive mixtures to those of the reactive mixtures for determining the volume profile for simulation purposes and of limiting the variation in T_c by limiting the uncertainty in the experimentally determined quantities that characterize the state of the mixture.

Declaration of Competing Interest

The authors declare that they have no known competing financial interests or personal relationships that could have appeared to influence the work reported in this paper.

Acknowledgments

L. Dai thanks the China Scholarship Council (CSC) for the financial support. P.G. would like to acknowledge funding from Orient's Fund.

Supplementary materials

Supplementary material associated with this article can be found, in the online version, at doi:10.1016/j.combustflame.2020.01.023.

References

[1] H. Kobayashi, A. Hayakawa, K.D.K.A. Somarathne, E.C. Okafor, Science and technology of ammonia combustion, Proc. Combust. Inst. 37 (2019) 109–133.
[2] J.M. Modak, Haber process for ammonia synthesis, Resonance 16 (2011) 1159–1167.
[3] C.W. Gross, S.C. Kong, Performance characteristics of a compression-ignition engine using direct-injection ammonia-DME mixtures, Fuel 103 (2013) 1069–1079.
[4] O. Kurata, N. Iki, T. Matsunuma, T. Inoue, T. Tsujimura, H. Furutani, H. Kobayashi, A. Hayakawa, Performances and emission characteristics of NH_3-air and NH_3-CH_4-air combustion gas-turbine power generations, Proc. Combust. Inst. 36 (2017) 3351–3359.
[5] E.C. Okafor, Y. Naito, S. Colson, A. Ichikawa, T. Kudo, A. Hayakawa, H. Kobayashi, Experimental and numerical study of the laminar burning velocity of CH_4–NH_3–air premixed flames, Combust. Flame 187 (2018) 185–198.
[6] E.C. Okafor, K.D.K.A. Somarathne, A. Hayakawa, T. Kudo, O. Kurata, N. Iki, H. Kobayashi, Towards the development of an efficient low-NO_x ammonia combustor for a micro gas turbine, Proc. Combust. Inst. 37 (2019) 4597–4606.
[7] O. Kurata, N. Iki, T. Inoue, T. Matsunuma, T. Tsujimura, H. Furutani, M. Kawano, K. Arai, E.C. Okafor, A. Hayakawa, H. Kobayashi, Development of a wide range–operable, rich-lean low-NO_x combustor for NH_3 fuel gas-turbine power generation, Proc. Combust. Inst. 37 (2019) 4587–4595.
[8] K. Takizawa, A. Takahashi, K. Tokuhashi, S. Kondo, A. Sekiya, Burning velocity measurements of nitrogen-containing compounds, J. Hazard. Mater. 155 (2008) 144–152.
[9] Y. Arakawa, R. Mimoto, T. Kudo, A. Hayakawa, H. Kobayashi, T. Goto, Laminar burning velocity and Markstein length of ammonia/air premixed flames at various pressures, Fuel 159 (2015) 98–106.
[10] Y. Song, H. Hashemi, J.M. Christensen, C. Zou, P. Marshall, P. Glarborg, Ammonia oxidation at high pressure and intermediate temperatures, Fuel 181 (2016) 358–365.
[11] H. Nakamura, S. Hasegawa, Combustion and ignition characteristics of ammonia/air mixtures in a micro flow reactor with a controlled temperature profile, Proc. Combust. Inst. 36 (2017) 4217–4226.
[12] H. Nakamura, S. Hasegawa, T. Tezuka, Kinetic modeling of ammonia/air weak flames in a micro flow reactor with a controlled temperature profile, Combust. Flame 185 (2017) 16–27.
[13] C. Brackmann, V.A. Alekseev, B. Zhou, E. Nordström, P.E. Bengtsson, Z. Li, M. Aldén, A.A. Konnov, Structure of premixed ammonia+air flames at atmospheric pressure: laser diagnostics and kinetic modeling, Combust. Flame 163 (2016) 370–381.
[14] P. Kumar, T.R. Meyer, Experimental and modeling study of chemical-kinetics mechanisms for H_2-NH_3-air mixtures in laminar premixed jet flames, Fuel 108 (2013) 166–176.
[15] J. Li, H. Huang, N. Kobayashi, C. Wang, H. Yuan, Numerical study on laminar burning velocity and ignition delay time of ammonia flame with hydrogen addition, Energy 126 (2017) 796–809.
[16] R. Li, A.A. Konnov, G. He, F. Qin, D. Zhang, Chemical mechanism development and reduction for combustion of $NH_3/H_2/CH_4$ mixtures, Fuel 257 (2019) 116059.
[17] X. Han, Z. Wang, M. Costa, Z. Sun, Y. He, K. Cen, Experimental and kinetic modeling study of laminar burning velocities of NH_3 /air, NH_3 /H_2 /air, NH_3 /CO/air and NH_3 /CH_4 /air premixed flames, Combust. Flame 206 (2019) 214–226.
[18] T. Takeyama, H. Miyama, A shock-tube study of the ammonia-oxygen reaction, Symp. Combust. 11 (1967) 845–852.
[19] J.N. Bradley, R.N. Butlin, D. Lewis, Oxidation of ammonia in shock waves, Trans. Faraday Soc. 64 (1968) 71–78.
[20] N. Fujii, M. Koshi, T. Asaba, N. City, Kinetics of ammonia oxidation in shock waves, Symp. (Int.) Combust. 18 (1981) 873–883.
[21] D.C. Bull, A shock tube study of the oxidation of ammonia, Combust. Flame 12 (1968) 603–610.
[22] H. Miyama, Kinetic studies of ammonia oxidation in shock waves IV. Comparison of induction periods for the ignition of NH_3-O_2-N_2 with those for NH_3-O_2-Ar mixtures, Bull. Chem. Soc. Japan 41 (1968) 1761–1765.
[23] L.J. Drummond, High temperature oxidation of ammonia, Combust. Sci. Technol. 5 (1972) 175–182.
[24] T. Takeyama, H. Miyama, Kinetic studies of ammonia oxidation in shock waves. III. The radiation of excited oh radicals, Bull. Chem. Soc. Jpn. 39 (1966) 2609–2612.
[25] O. Mathieu, E.L. Petersen, Experimental and modeling study on the high-temperature oxidation of Ammonia and related NO_x chemistry, Combust. Flame 162 (2015) 554–570.
[26] B. Shu, S.K. Vallabhuni, X. He, G. Issayev, K. Moshammer, A. Farooq, R.X. Fernandes, A shock tube and modeling study on the autoignition properties of ammonia at intermediate temperatures, Proc. Combust. Inst. 37 (2019) 205–211.
[27] M. Pochet, V. Dias, B. Moreau, F. Foucher, H. Jeanmart, F. Contino, Experimental and numerical study, under LTC conditions, of ammonia ignition delay with and without hydrogen addition, Proc. Combust. Inst. 37 (2018) 621–629.
[28] X. He, B. Shu, D. Nascimento, K. Moshammer, M. Costa, R.X. Fernandes, Auto-ignition kinetics of ammonia and ammonia/hydrogen mixtures at intermediate temperatures and high pressures, Combust. Flame 206 (2019) 189–200.
[29] P. Glarborg, J.A. Miller, B. Ruscic, S.J. Klippenstein, Modeling nitrogen chemistry in combustion, Prog. Energy Combust. Sci. 67 (2018) 31–68.
[30] S.J. Klippenstein, L.B. Harding, P. Glarborg, J.A. Miller, The role of NNH in NO formation and control, Combust. Flame 158 (2011) 774–789.
[31] K.P. Shrestha, L. Seidel, T. Zeuch, F. Mauss, Detailed kinetic mechanism for the oxidation of ammonia including the formation and reduction of nitrogen oxides, Energy Fuels 32 (2018) 10202–10217.
[32] S. Gersen, A.V. Mokhov, J.H. Darmeveil, H.B. Levinsky, Ignition properties of n-butane and iso-butane in a rapid compression machine, Combust. Flame 157 (2010) 240–245.
[33] S. Gersen, A.V. Mokhov, J.H. Darmeveil, H.B. Levinsky, P. Glarborg, Ignition-promoting effect of NO_2 on methane, ethane and methane/ethane mixtures in a rapid compression machine, Proc. Combust. Inst 33 (2011) 433–440.
[34] P. Park, J.C. Keck, Rapid compression machine measurements of ignition delays for primary reference fuels, SAE Tech. Pap., SAE International, 1990.
[35] S. Gersen, Experimental Study of the Combustion Properties of Methane / Hydrogen Mixtures Ph.D. Thesis, University of Groningen, 2007.
[36] S.J. Klippenstein, L.B. Harding, B. Ruscic, R. Sivaramakrishnan, N.K. Srinivasan, M.C. Su, J.V. Michael, Thermal decomposition of NH_2OH and subsequent reactions: ab initiotransition state theory and reflected shock tube experiments, J. Phys. Chem. A 113 (2009) 10241–10259.

[37] P. Van Khe, J.C. Soulignac, R. Lesclaux, Pressure and temperature dependence of NH_2 recombination rate constant, J. Phys. Chem. 81 (1977) 210–214.
[38] V.A. Lozovskii, V.A. Nadtochenko, O.M. Sarkisov, S.G. Cheskis, Study of NH_2 radical recombination by intraresonator laser spectroscopy, Kinet. Catal. 20 (1979) 918–922.
[39] O.M. Sarkisov, S.G. Cheskis, V.A. Nadtochenko, E.A. Sviridenkov, V.I. Vedeneev, Spectroscopic study of elementary reactions involving HCO, NH_2 and HNO, Arch. Combust. 4 (1984) 111–120.
[40] K. Fagerström, J.T. Jodkowski, A. Lund, E. Ratajczak, Kinetics of the self-reaction and the reaction with OH of the amidogen radical, Chem. Phys. Lett. 236 (1995) 103–110.
[41] G. Altinay, R.G. MacDonald, Determination of the rate constant for the NH_2(X 2B 1) + NH_2 (X 2B 1) recombination reaction with collision partners He, Ne, Ar, and N_2 at low pressures and 296 K. Part 1, J. Phys. Chem. A 116 (2012) 1353–1367.
[42] R.W. Diesen, Mass spectral studies of kinetics behind shock waves. II. Thermal decomposition of hydrazine, J. Chem. Phys. 39 (1963) 2121–2128.
[43] E. Meyer, H.A. Olschewski, J. Troe, H.G. Wagner, Investigation of N_2H_4 and H_2O_2 decomposition in low and high pressure shock waves, Symp. Combust., Elsevier (1969), pp. 345–355.
[44] P. Genich, A.A. Zhirnov, G.B. Manelis, Decomposition of hydrazine behind reflected shock waves at high pressures, Zh, Phys. Khim. 48 (1974) 728–729.
[45] O.V. Dorofeeva, O.N. Ryzhova, T.A. Suchkova, Enthalpies of formation of hydrazine and its derivatives, J. Phys. Chem. A. 121 (2017) 5361–5370.
[46] D. Feller, D.H. Bross, B. Ruscic, Enthalpy of formation of N_2H_4 (Hydrazine) revisited, J. Phys. Chem. A. 121 (2017) 6187–6198.
[47] D.G. Goodwin, H.K. Moffat, R.L. Speth, Cantera: an object-oriented software toolkit for chemical kinetics, thermodynamics, and transport processes. version 2.3.0, (2017).
[48] U. Burke, K.P. Somers, P. O'Toole, C.M. Zinner, N. Marquet, G. Bourque, E.L. Petersen, W.K. Metcalfe, Z. Serinyel, H.J. Curran, An ignition delay and kinetic modeling study of methane, dimethyl ether, and their mixtures at high pressures, Combust. Flame 162 (2015) 315–330.
[49] Y. Wu, Y. Liu, C. Tang, Z. Huang, Ignition delay times measurement and kinetic modeling studies of 1-heptene, 2-heptene and n-heptane at low to intermediate temperatures by using a rapid compression machine, Combust. Flame 197 (2018) 30–40.
[50] S. Tanaka, F. Ayala, J.C. Keck, J.B. Heywood, Two-stage ignition in HCCI combustion and HCCI control by fuels and additives, Combust. Flame 132 (2003) 219–239.
[51] H. Wu, Z. Shi, C. Lee, H. Zhang, Y. Xu, Experimental and kinetic study on ignition of DME/ n-butane mixtures under high pressures on a rapid compression machine, Fuel 225 (2018) 35–46.